Available online at www.sciencedirect.com
ScienceDirect
Renewable Energy 33 (2008) 906–913
RENEWABLE ENERGY
www.elsevier.com/locate/renene

Static and dynamic wind turbine simulator using a converter controlled dc motor

Mohammad Monfared[a], Hossein Madadi Kojabadi[b,*], Hasan Rastegar[a]

[a]Department of Electrical Engineering, Amirkabir University of Technology, Tehran, Iran
[b]Department of Electrical Engineering, Sahand University of Technology, Tabriz 51335-1996, Iran

Received 24 January 2007; accepted 3 June 2007
Available online 23 August 2007

Abstract

This paper describes a new wind turbine simulator for dynamic conditions. The authors have developed an experimental platform to simulate the static and dynamic characteristics of real wind energy conversion system. This system consists of a 3 kW dc motor, which drives a synchronous generator. The converter is a 3 kW single-phase half-controlled converter. MATLAB/Simulink real time control software interfaced to I/O board and a converter controlled dc motor are used instead of a real wind turbine. A MATLAB/Simulink model is developed that obtains wind profiles and, by applying real wind turbine characteristics in dynamics and rotational speed of dc motor, calculates the command shaft torque of a real wind turbine. Based on the comparison between calculated torques with command one, the shaft torque of dc motor is regulated accordingly by controlling armature current demand of a single-phase half-controlled ac–dc converter. Simulation and experimental results confirm the effectiveness of proposed wind turbine simulator in emulating and therefore evaluating various turbines under a wide variety of wind conditions.
© 2007 Elsevier Ltd. All rights reserved.

Keywords: AC–DC power conversion; DC motor drives; Dynamics; Wind energy

1. Introduction

A wind turbine emulator (WTE) is an important equipment for developing wind energy conversion systems. This emulator simulates steady-state and dynamic behaviors in a controlled environment without reliance on natural wind resources and actual wind turbines, for the purpose of R&D into wind turbine drive trains, especially energy conversion systems. The emulator can be used for research applications to drive an electrical generator in a similar way as a wind turbine, by reproducing the torque developed by a wind turbine for a given wind velocity. Also, it can be used as an educational tool to teach the behavior, operation and control of a wind turbine.

In the past few years there have been various studies on wind turbine simulators (WTSs). Authors of [1–3] utilized separately excited dc motors with controlled armature current. Ref. [1] presented a WTS using the electromagnetic (EM) torque equation of a dc machine. The armature and the field circuits were controlled so that the dc machine generated the static characteristics of a constant pitch wind turbine. In [4,5] for the first time IGBT inverter controlled IM has been used as a WTS. The armature current and frequency demand values were controlled in such a way that the IM shaft generated the steady-state characteristics of a constant pitch wind turbine. In order to have accurate study on wind turbine behavior having tower shadow and larger turbine inertia effects is necessary. For the first time tower shadow effect of wind turbine has been added to real wind turbine modeling in [6]. The emulator reproduced the mean torque of the turbine and the oscillating torque due to wind shear and tower shadow without taking into consideration the large turbine inertia in modeling. In Ref. [7] even though the dynamic effects of a large turbine inertia and tower shadow have been modeled but the effect of gear ratio for inertia and torque has been omitted, in other words the gear ratio is considered as unit that is not the case in real world. Dolan et al. in [8] modeled the torque oscillations caused by wind shear, tower shadow,

*Corresponding author. Tel./fax: +98 411 3808208.
E-mail address: hmadadi64@yahoo.ca (H. Madadi Kojabadi).

0960-1481/$ - see front matter © 2007 Elsevier Ltd. All rights reserved.
doi:10.1016/j.renene.2007.06.007

and the obvious pulsations caused by variable wind speed. But they failed to include the dynamic effects of a larger turbine inertia since the ratio of PMSM inertia to generator inertia has been chosen as approximately two. This nearly eliminates the effect of a large rotor inertia that would be seen in real systems. Meanwhile their model needs torque transducer to determine what compensation is required to emulate the driving torque of the wind turbine and inertial dynamics. Also the steady-state characteristics of real wind turbine have not been presented as they claimed in abstract. Permanent magnet dc motor has been used in [9]. This paper presents an improved version that considers the harmonic torques due to the gradient and tower shadow effects, and inertia of the wind turbine drive train. The shaft mechanical model of the real wind turbine is distinctly different from the simulator system in which the real wind turbine shaft is replaced by a dc motor shaft. Obviously these two systems have different inertias, friction coefficients and elasticity. So the dynamic equations presented in [9] for rotational shafts not only do not improve the dynamic accuracy of the simulator but also these may lead to much worse results than ignoring the elasticity and friction. On the other hand, modeling the turbine shaft elasticity while assuming a rigid coupling between the generator and the motor has no advantages. Meanwhile, the effect of large turbine inertia has not been clearly presented in dynamic equations of WTE. In [11], a microcomputer-controlled SCR-DC motor was used to supply the shaft torque. This emulator only contains steady-state behavior of a real wind turbine. Tower shadow and larger turbine inertia to DC motor shaft inertia effects are usually neglected [10].

The WTE described in this paper aims to reproduce the mechanical behavior of the wind turbine rotor, drive train and a gear box under dynamic conditions. The reference for the torque developed by the wind turbine includes the gradient and tower shadow effects that result in pulsating torques. The larger inertia effect and the steady-state behavior of real wind turbine such as $C_p-\lambda$ and P_m-n characteristics are also included in this emulator. It is important to mention that WTEs with some of these characteristics have been discussed in the literature before but they were not described in details to allow their easy replication [6–13]. The emulator/simulator outlined in this paper includes several important components of which one or more was missing in other simulators. These components are: a variable wind speed, turbine inertia and a wind shear, tower shadow model, and steady-state characteristics. One of the most important goals of this paper is to find very easy way for dynamic behavior description of real wind turbine for electrical engineers and researchers including the torque oscillations caused by wind shear, tower shadow, the obvious pulsations caused by variable wind speed, and the dynamic effects of a large turbine inertia. To do this we used MATLAB/Simulink software that includes all the necessary blocks in detail for dynamic modeling of real wind turbine, also its real time windows target toolbox provides sufficient tools for exchanging data with interface hardware.

2. Emulator construction

The emulator is based on the energy conversion system shown in Fig. 1. The laboratory system is realized by replacing the wind, gearbox and turbine rotor with a PC, ac–dc converter, dc drive, and dc motor as shown in Fig. 2. The PC implementing MATLAB/Simulink uses a wind shear/tower shadow model, an inertia model, steady-state characteristics, and a variable wind to control the dc system to emulate the driving torque of a wind turbine. These models will be briefly outlined as well as the computer hardware components along with the drive equipments and control methodology used.

2.1. Tower shadow/wind shear model

In order to increase the emulator reliability and to avoid the delay time of torque transducer and also to reduce the overall cost of the simulator the dc motor torque will be estimated. Since this torque has been calculated from dc motor current in order to have accurate torque calculation the dc motor losses such as copper and rotational losses will be added to calculated power of wind profile. As a turbine blade rotates, it is acted upon by wind at various heights. The variation of wind speed with height is termed wind shear. Wind speed generally increases with height. Torque pulsations, and therefore power pulsations, are observed due to the periodic variations of wind speed experienced at different heights. Power and torque oscillate due to the different wind speeds encountered by each blade as it rotates through a complete cycle. For instance, a blade pointing upwards would encounter wind speeds greater than a blade pointing downwards. During each rotation the torque oscillates three times because of each blade passing through minimum and maximum wind. To determine control structures and possible power quality issues, the dynamic torque generated by the blades of a wind turbine must be represented. It is therefore important to model these wind shear and tower shadow induced 1P and 3P torque pulsations for a meaningful WTE as [9]

$$T_{mech} = T_{mill}[1 + A_1 \sin(\omega_{mill} t) + A_3 \sin(3\omega_{mill} t)], \tag{1}$$

where $A_1 = 0.2$ and $A_3 = 0.4$, T_{mill} and T_{mech} are average and aerodynamic torques of wind turbine, respectively. The

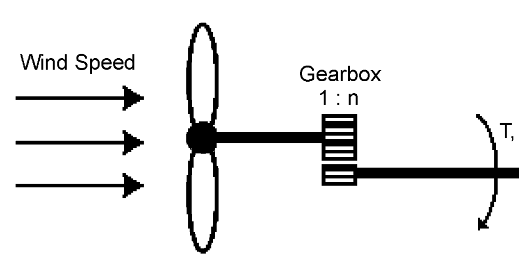

Fig. 1. Wind turbine system.

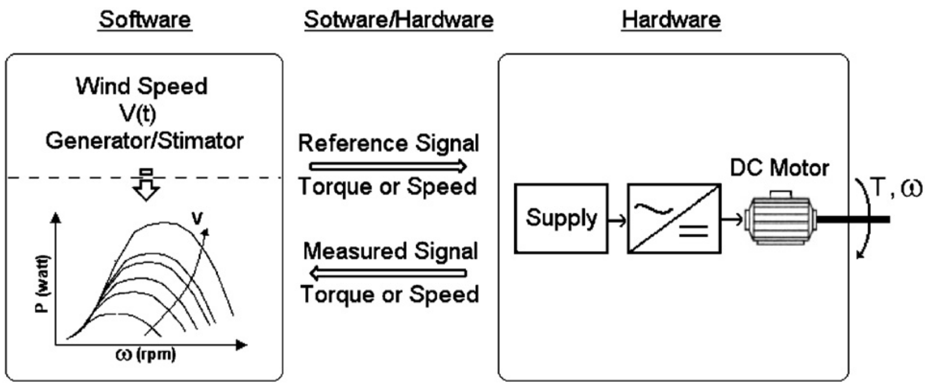

Fig. 2. Wind turbine simulator system.

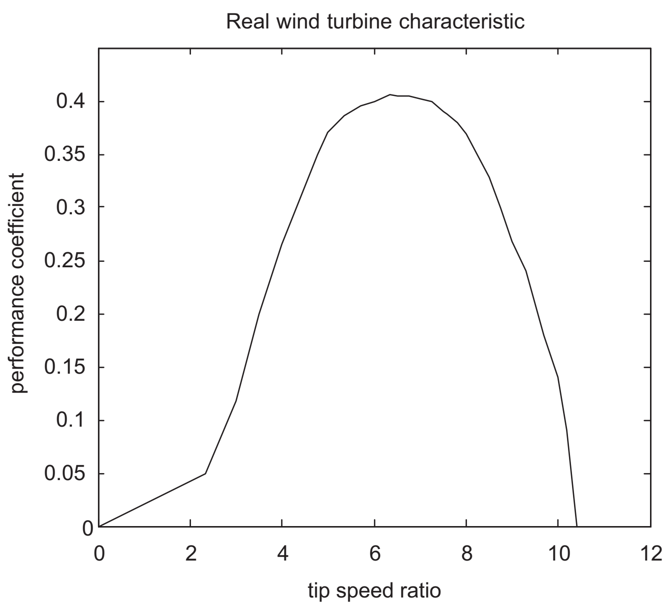

Fig. 3. C_p–λ characteristic of a real wind turbine.

average power and torque developed by a wind turbine are a function of the wind speed (u), the rotational speed of the shaft (ω_{mill}), the tip-speed ratio (λ) and the torque and power coefficients (C_q and C_p) as given by (2) and (3) where r_m is the radius of the turbine and ρ is the air density:

$$P_{\text{mill}} = 0.5 \times \rho\pi r_m^2 C_P u^3, \tag{2}$$

$$T_{\text{mill}} = 0.5 \times \rho\pi r_m^3 C_q u^2 \tag{3}$$

and,

$$\lambda = \frac{r_m n\pi}{30u}. \tag{4}$$

The C_p, power coefficient versus λ, tip speed ratio curve shown in Fig. 3 and used in this paper was obtained from [4,5].

2.2. Inertia compensation

The inertia model is determined by equating the generator acceleration in the field and lab systems. The effect is to alter the turbine torque that the dc motor will produce in response to a given wind, such that the effect of the larger turbine rotor inertia is emulated. A mechanical diagram of both the field system and the representative laboratory system is shown in Fig. 4, where T_{motor} is the dc motor's torque, T_{mech} the aerodynamic turbine rotor torque, T_{gen} the generator torque, J_{motor} the dc motor inertia, J_g the generator inertia, and J_{mill} the turbine rotor inertia. Equations of motion may be written for both systems, real wind turbine (5) and simulator (6) and solved to determine the reference torque (7) required for the dc motor:

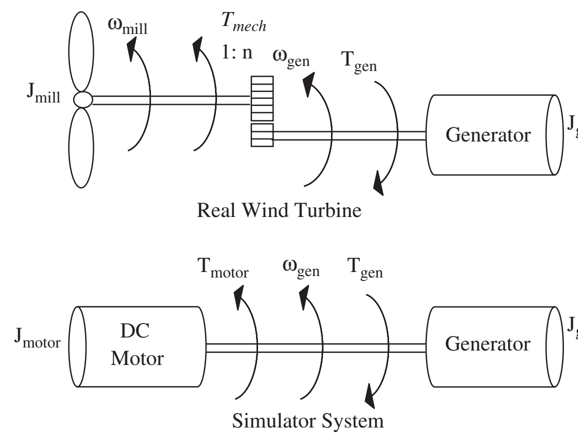

Fig. 4. Mechanical models of real and simulated WT.

$$\frac{T_{\text{mech}}}{n} = \left(\frac{J_{\text{mill}}}{n^2} + J_g\right)\frac{d\omega_{\text{gen}}}{dt} + T_{\text{gen}}, \tag{5}$$

$$T_{\text{motor}} = (J_{\text{motor}} + J_g)\frac{d\omega_{\text{gen}}}{dt} + T_{\text{gen}}, \tag{6}$$

$$T_{\text{motor}} = \frac{T_{\text{mech}}}{n} + \left(J_{\text{motor}} - \frac{J_{\text{mill}}}{n^2}\right)\frac{d\omega_{\text{gen}}}{dt}, \tag{7}$$

where n is gear ratio and the second term of right-hand side of (7) represents the compensation torque of WTE. Therefore the WTE will accurately represent the field wind turbine system if the driving torque T_{motor} is controlled according to (7). Fig. 5 shows the wind turbine simulation

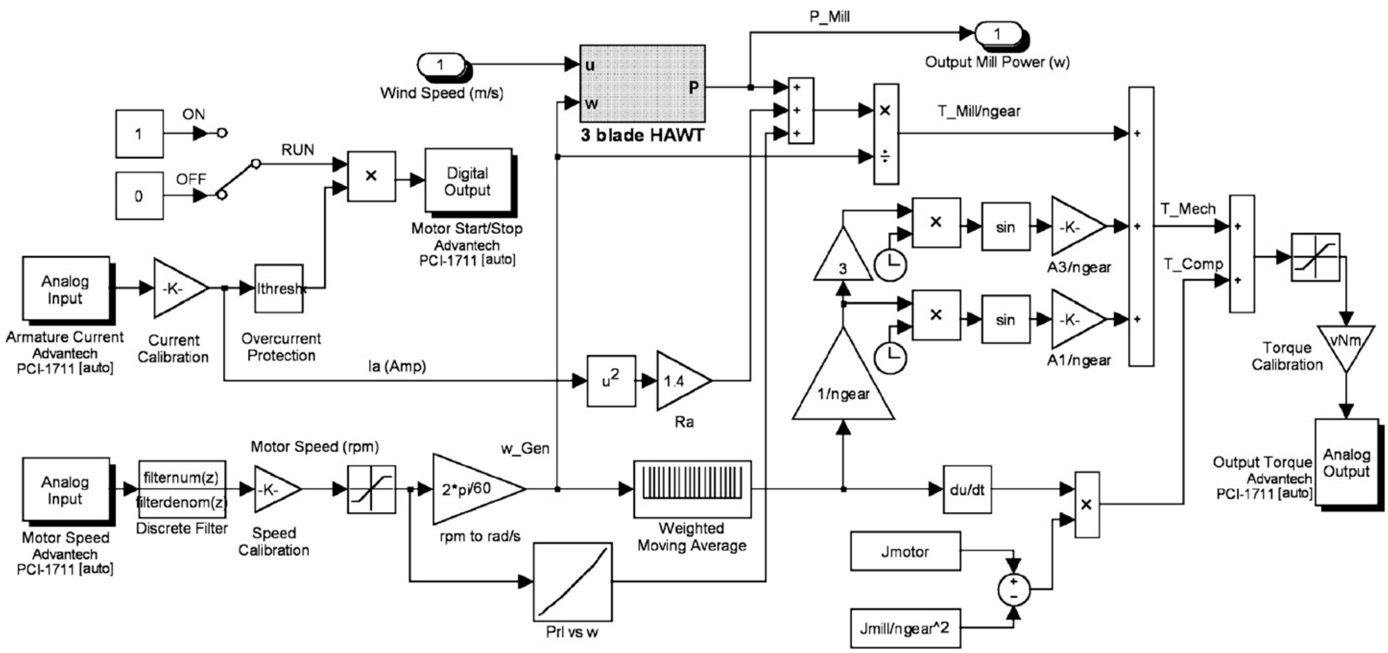

Fig 5. Wind turbine simulation block diagram.

block diagram which consists of torque calculation block, torque pulsations due to wind shear and tower shadow effects and compensation torque effect due to larger turbine inertia.

3. System implementation

A 3 kW, 220 V and 1500 rpm dc motor was used in the WTE prototype. The gear box ratio and the radius of the emulated wind turbine were selected as 25:1 and 4.5 m, respectively, so that the dc motor torque and speed values remain within rated values. The maximum speed for the wind turbine becomes 1 rps. Therefore, the bandwidth required from the current control loop so that the WTE can reproduce a torque with the gradient and the tower shadow effects is equal to 3 Hz. The single-phase half-controlled drive used in this emulator for dc motor control as shown in Fig. 6 produces harmonics (ripples) with 100 Hz that are outside the required bandwidth of gradient and the tower shadow effects of 3 Hz. The sampling frequency of emulator has been chosen 100 Hz that this is equal to ripples produced by converter, so with this sampling frequency the harmonics produced by converter will be avoided.

3.1. Steady-state characteristics of WT

The wind turbine model and the digital PID controller are developed on a MATLAB/Simulink platform for easy access, programming and modifications realized using a PC interfaced to Data Acquisition Interface I/O board. This I/O system is equipped with 8 A/D channels and 2 D/A channels for control and acquisition purposes. The

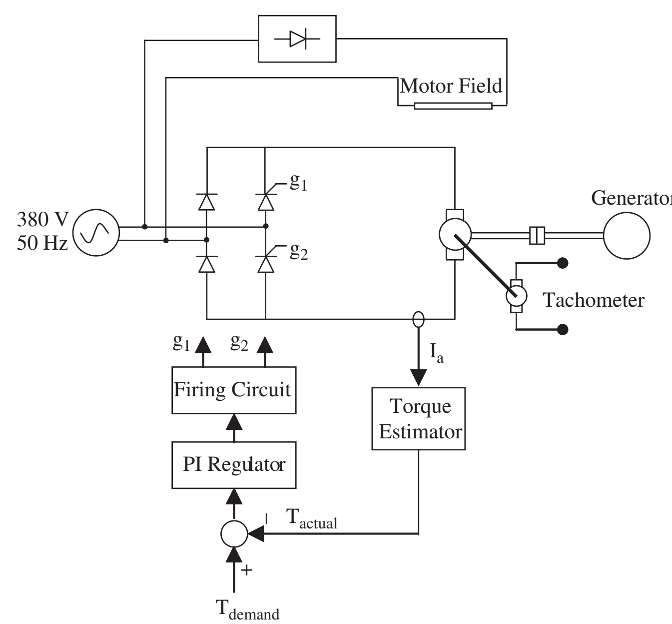

Fig. 6. Single-phase half-controlled drive.

controller generates the current demand for the single-phase half-controlled converter drive. In this research a horizontal axis wind turbine as described by Fig. 3 is used. The parameters of dc motor and wind turbine are listed in Tables 1 and 2, respectively. The power-speed characteristics of WTS at different wind speeds as measured during tests are shown in Fig. 7, and are compared with those of a real wind turbine. Based on (3) and (4), the $C_p-\lambda$ characteristic can be derived from the measured P_m-n characteristics of Fig. 7. The measured $C_p-\lambda$ characteristic

Table 1
Parameters of dc motor

Field	220 V/0.7 A
Rated power (kW)	3
Nominal speed (rpm)	1500
J (kg m^2)	0.25
R_a (Ω)	1.4
L_a (mH)	27

Table 2
Parameters of wind turbine

Gearbox ratio	25
J (kg m^2)	7
Rated power (kW)	2.5
Rotor radius (m)	4.5

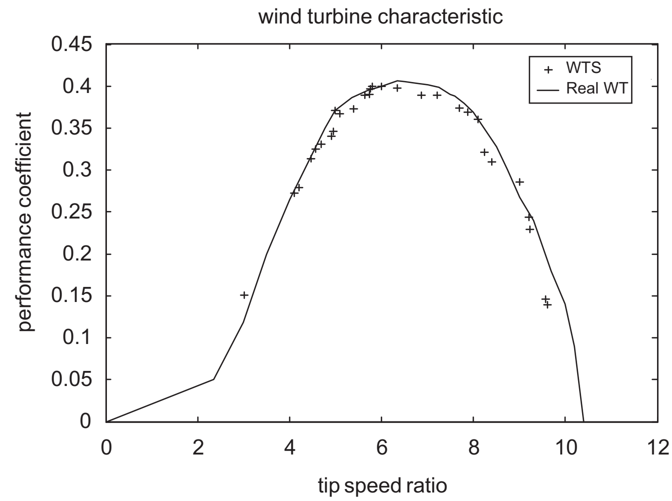

Fig. 8. C_p–λ characteristics of a real WT and WTS.

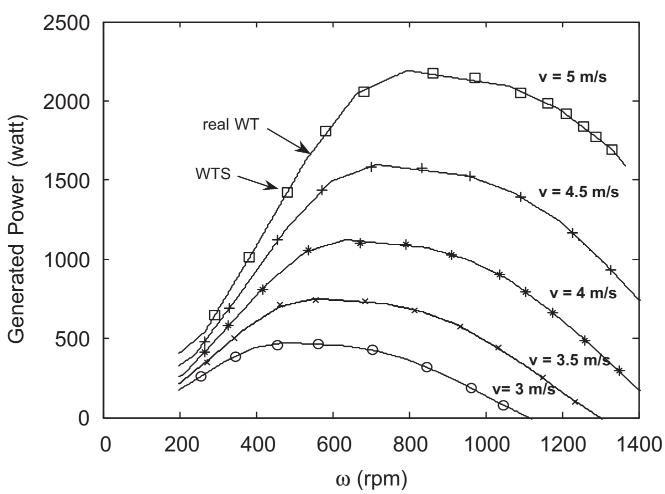

Fig. 7. Tested power-speed characteristics of a WTS.

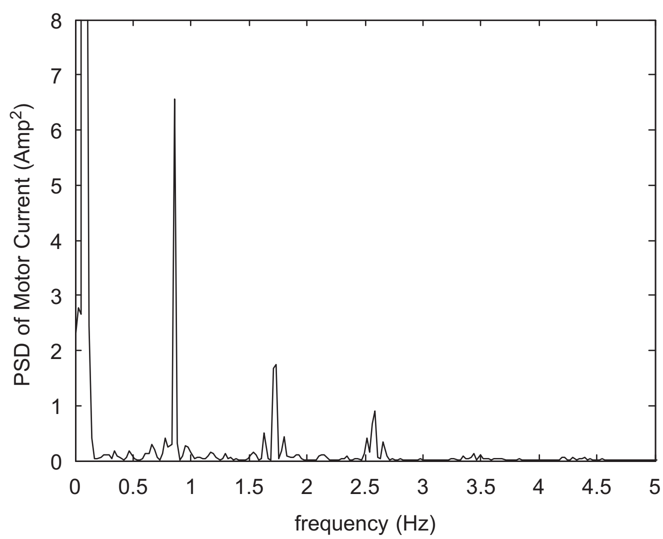

Fig. 9. Frequency spectrum of the motor current considering the pulsating torques ($J = 0.25$ kg m^2).

is compared with that of the wind turbine given in Fig. 3, as presented in Fig. 8. Both Figs. 7 and 8 verifies that the developed WTS reproduces the steady-state characteristics of a given wind turbine at various wind conditions accurately.

3.2. Dynamic behavior of WT

3.2.1. Tower shadow and wind shear effects

The turbine torque oscillations due to tower shadow and wind shear were calculated based on the turbine specifications. These oscillations were sufficient to cause a resultant fluctuation in the output current, such that the effects due to tower shadow could easily be distinguished in the time domain. For this purpose we apply constant wind speed such that the generator shaft speed rises to 1319 rpm. Since the gear ratio is 1:25 so the 1P and 3P frequency of oscillations due to tower shadow and wind shear effects can be calculated as

$$1\text{P} = \frac{1310}{60 \times 25} \approx 0.87\,\text{Hz},$$
$$3\text{P} = 3 \times 1\text{P} \approx 2.6\,\text{Hz} \tag{8}$$

Figs. 9 and 10 show frequency spectrum induced in motor current and output power of simulator for $J = 0.25\,\text{kgm}^2$, respectively. Fig. 11 shows the frequency spectrum of motor current without tower shadow effects. From Fig. 10 it is clear that the magnitudes of 1P and 3P harmonics significantly deteriorated. This is because of low pass filter behavior of wind turbine. Based on (9) the natural damping frequency of wind turbine is near to 1P and 3P:

$$f_D = \sqrt{\frac{\omega_0 K}{8\pi^2} \times \frac{J_{\text{mill}} + J_E}{J_{\text{mill}} J_E}} \times \sqrt{1 - D^2}, \tag{9}$$

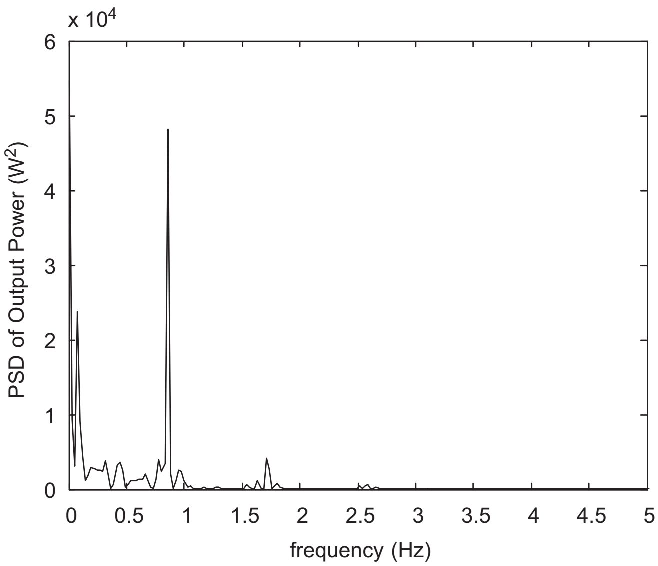

Fig. 10. Frequency spectrum of the simulator output power considering the pulsating torques ($J = 0.25\,\mathrm{kg\,m^2}$).

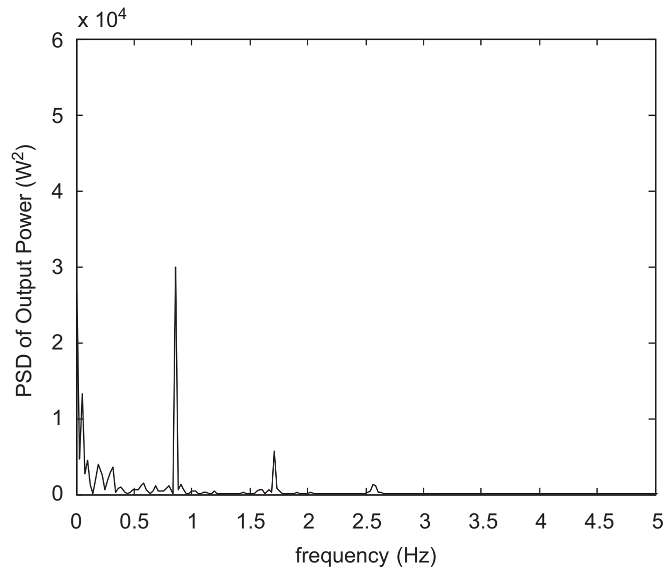

Fig. 12. Frequency spectrum of the simulator output power considering pulsating torques and larger inertia ($J = 7\,\mathrm{kg\,m^2}$).

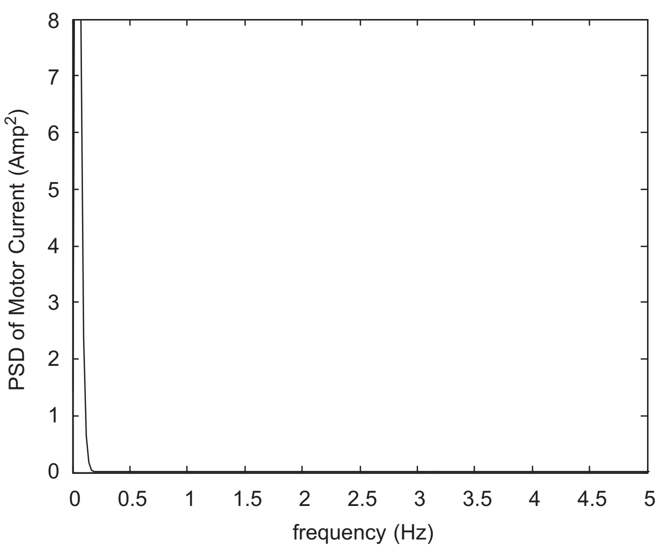

Fig. 11. Frequency spectrum of the motor current ignoring the pulsating torques ($J = 0.25\,\mathrm{kg\,m^2}$).

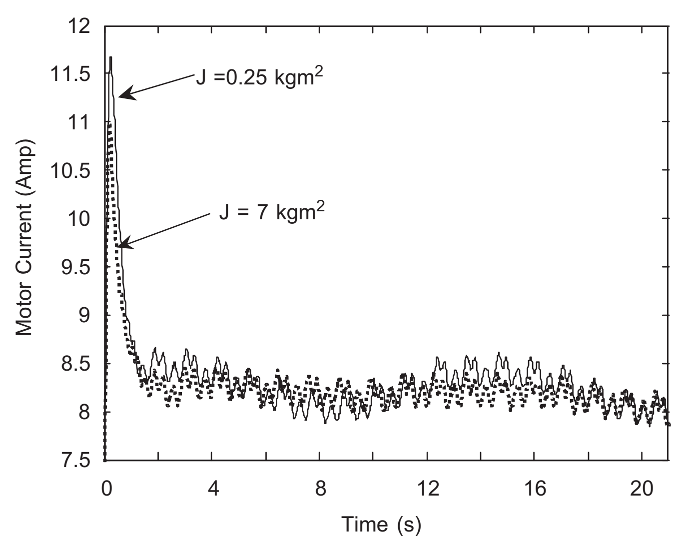

Fig. 13. Transient response of the motor current including larger inertia effect and a step variation of the wind speed.

where D is system damping, ω_0 is system speed, and J_{mill} and J_{g} are the inertia of the wind turbine and the generator, respectively, K is the shaft stiffness.

3.2.2. Inertia model

The inertia model is determined by equating the generator acceleration in the field and laboratory systems. The effect is to alter the turbine torque that the dc motor will produce in response to a given wind, such that the effect of the larger turbine rotor inertia is emulated. Frequency spectrum of the simulator output power including tower shadow and wind shear effects and larger inertia ($J = 7\,\mathrm{kg\,m^2}$) is shown in Fig. 12. By comparing Figs. 10 and 12 one can see that the turbine with larger inertia demonstrates reduced magnitude for 1P and 3P harmonics. Fig. 13 shows the motor current transient for different values of moment of inertia for the wind turbine.

From this figure it is clear that the rotor with higher value of inertia yielded reduced oscillations and low overshoot in motor current. Fig. 14 shows how the wind turbine speed developed by the WTE varies for different values of moment of inertia ($J = 0.25$, and $7\,\mathrm{kg\,m^2}$) for the wind turbine. One can see that rotors with higher values of moment of inertia yield reduced oscillations in the shaft and slower dynamics. From (9) it is clear that the higher

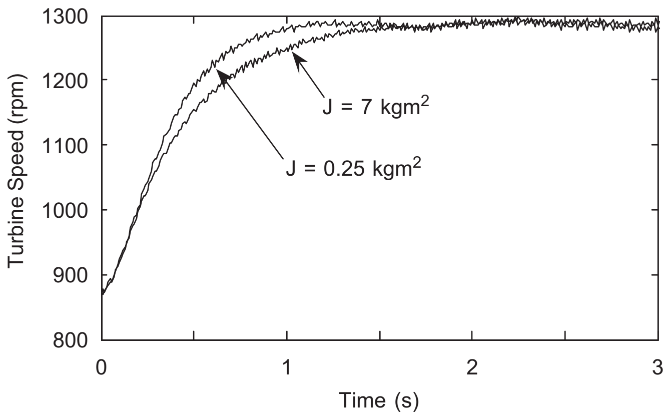

Fig. 14. Effect of J on the transient response of the turbine speed following a step variation of the wind speed.

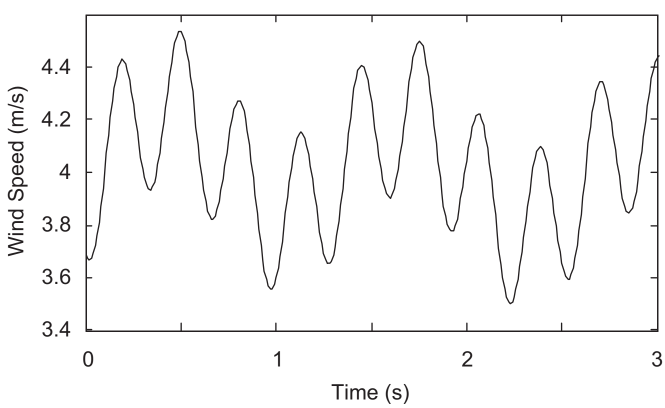

Fig. 15. Reference wind speed applied to simulator.

inertia resulted in lower natural damping frequency as

$$\frac{f_{D(J=0.25)}}{f_{D(J=7)}} \approx 1.4.$$

3.2.3. Turbulent wind speed

In order to evaluate the performance of proposed emulator in turbulent wind speed condition an experimental test has been carried out. Wind speed versus time is shown in Fig. 15. Frequency spectrum of applied wind speed is shown in Fig. 16. One can see that the wind speed has the harmonics of 0.8, 3.2, and 15.9 Hz. Frequency spectrum of the dc motor current due to oscillating wind speed and larger turbine inertia is shown in Fig. 17. From this figure it is clear that due to low pass filter behavior of wind turbine which its cutting frequency in this case is about 2.5 Hz, the 15.9 Hz harmonic has been disappeared in frequency spectrum of the dc motor current due to oscillating wind speed also the 3.2 Hz is significantly damped. Fig. 18 shows variable wind speed effects on turbine speed for different values of moment of inertia. Larger turbine inertia reduces the magnitude of oscillations in turbine speed. The bandwidth of the emulator torque

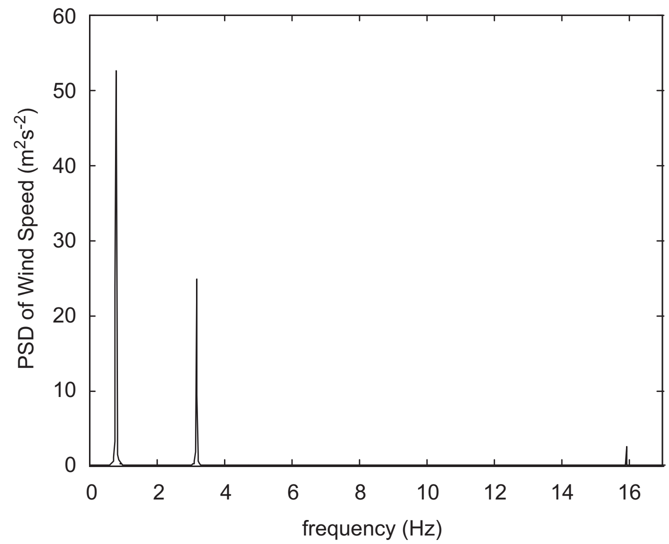

Fig. 16. Frequency spectrum of the wind speed.

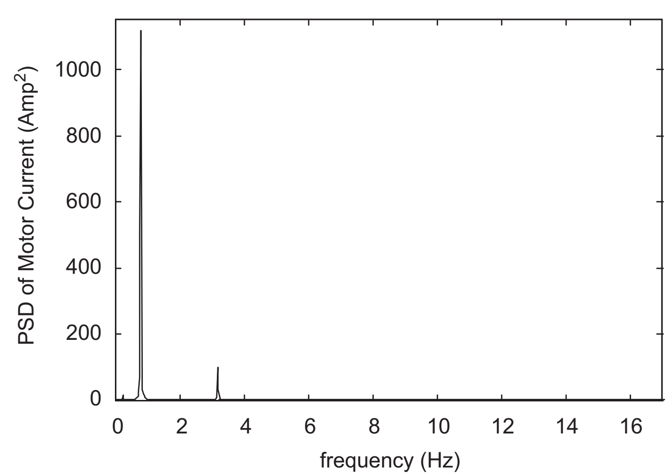

Fig. 17. Frequency spectrum of the dc motor current due to oscillating wind speed and larger turbine inertia ($J = 7\,kg\,m^2$).

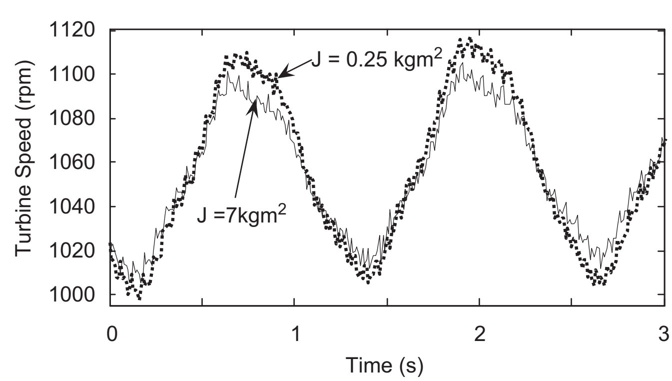

Fig. 18. Effects of wind speed variations and larger inertia in turbine speed.

control loop is determined to be about 3 Hz. In fact, for sinusoidal ripples with frequencies above 3 Hz, the magnitude of the actual armature current decreases and the phase delay increases considerably compared to the reference values. Based on (9), a real wind turbine system behaves like a low pass filter while its natural damping frequency f_D, depends upon D, K, and J. For large wind turbines, J_{mill} is big enough so that f_D usually becomes smaller than the emulator bandwidth. In these cases the emulator performance in turbulent wind is not limited. In other words, larger wind turbines due to their smaller f_D will prevent the appearance of high frequencies in their output power spectrum. However, when small wind turbines are studied, it is more likely that f_D exceeds the emulator bandwidth. Here, some higher frequencies which are expected to be appeared in the real wind turbine output due to the turbulent wind may not be represented efficiently by the emulator system.

4. Conclusion

In order to improve the effectiveness and efficiency of research into wind energy conversion systems, a dc motor based WTS has been developed to create a controlled test environment for drive train of wind turbines. The wind turbine model and the digital controller are developed on a MATLAB/Simulink platform for easy access, programming and modification. Various wind turbines and wind profiles can be incorporated in the control software. In this paper very accurate and detailed dynamic behavior of real wind turbine has been introduced. The simulator outlined in this paper includes several important components of real wind turbine including, wind shear and tower shadow effects, larger turbine inertia, turbulent wind speed, and steady-state characteristics which one or more was missing in other simulators. Various tests conducted on the developed WTS and the resultant responses of a variety of WTS parameters have confirmed the good performance of the WTS under the designed digital controllers.

References

[1] Nunes AAC, Seixa PF, Cortizo PC, Silva SR. Wind turbine simulator using a dc machine and a power reversible converter. In: Proceedings of the international conference on electrical machines. ICEMA, vol. 3. Adelaide, Australia, 1993. p. 536–40.

[2] Battaiotto PE, Mantz RJ, Puleston PF. A wind turbine emulator based on a dual DSP processor system. Control Eng Practice 1996;4(9):1261–6.

[3] Rodriguez-Amenedo JL, Rodriguez Garcia F, Chincilla JC, Veganzones C. Experimental rig to emulate wind turbines. In: Proceedings of the international conference on electrical machines. ICEM 98, vol. 3. Istanbul, Turkey, 1998. p. 2033–8.

[4] Madadi Kojabadi H, Chang L. A novel steady state wind turbine simulator using an inverter controlled induction motor. Wind Eng 2004;28(4):433–46.

[5] Madadi Kojabadi H, Chang L, Bouot T. Development of a novel wind turbine simulator for wind energy conversion systems using an inverter-controlled induction motor. IEEE Trans Energy Convers 2004;19(3):547–52.

[6] Chinchilla M, Arnaltes S, Rodriguez-Arnenedo JL. Laboratory set-up for wind turbine emulation. In: IEEE International Conference Industrial Technology. vol. 1. 8–10 December. p. 553–7.

[7] Seung-Ho S, Byoung-Chang J, Hye-In L, Jeong-Jae K, Jeong-Hun O, Venkataramanan G. Emulation of output characteristics of rotor blades using a hardware-in-loop wind turbine simulator. In: 12th annual IEEE conference and Exposition Applied Power Electronics, APEC 2005, vol. 3. 6–10 March 2005. p. 1791–6

[8] Dolan Dale SL, Lehn PW. Real-time wind turbine emulator suitable for power quality and dynamic control studies. In: International conference on power systems transients (IPST'05). Montreal, Canada, 19–23 June 2005. p. 1–6

[9] Lopes LAC, Lhuilier J, Mukherjee A, Khokar MF. A wind turbine emulator that represents the dynamics of the wind turbine rotor and drive train. In: 36th IEEE conference on power electronics specialists, 12 Jun 2005. p. 2092–7.

[10] Nichita C, Diop AD, Elhache J, Dakyo B, Protin L. Control structures analysis for a real wind system simulator. Wind Eng 1998;22(6):275–86.

[11] Jian L, Xu WC. The simulation system of wind turbine performance using a microcomputer controlled SCR-DC motor. In: Proceedings of the Beijing International Conference on Electrical Machines, Beijing, China, 1987. p. 865–8.

[12] Teodorescu R, Iov F, Blaabjerg F. Flexible development and test system for a 11 kW wind turbine. In: Proceedings of 34th IEEE power electronics specialists conference (PESC03). vol. 1. June 2003. p. 67–72.

[13] Rabelo B, Hofmann W, Gluck M. Emulation of the static and dynamic behavior of a wind turbine with a DC machine. In: Proceedings of 35th IEEE power electronics specialists conference (PESC-05), June 2004. p. 107–2112.